Characterizing AFM Tip Lateral Positioning Variability Through Non-Vector Space Control-Based Nanometrology

Zhiyong Sun, *Member, IEEE*, Yu Cheng, *Member, IEEE*, Ning Xi, *Fellow, IEEE*, Ruiguo Yang, *Member, IEEE*, Yongliang Yang, Liangliang Chen, and Bo Song, *Member, IEEE*

***Abstract*—Atomic force microscopy (AFM) based nanotechnology has been widely implemented in various fields for decades in light of its overwhelming advantages, such as nanometer spatial resolution, adaptability to liquid ambient, and various nanomechanical/electrical metrological approaches. It is noted that though AFM possesses imaging capability up to nanometer resolution, it is hard to achieve nanometer level positioning precision due to the existing system variability, especially the thermal drift, which distorts AFM images through relatively long capturing time. Since an AFM image is typically utilized as a global reference map to navigate its tip to the desired locations for precise measurement and manipulation, the system variability distorted image will definitely diversify the experimental results. Therefore, it is necessary to characterize the positioning variability for better experimental results evaluation and decision-making. Although various approaches were proposed to evaluate AFM positioning error, to our best knowledge, there is little research about characterizing its positioning variability precisely and systematically. In this study, we present a universal metrological approach to quantitatively measure AFM tip locating variability by developing a featureless spiral local scan strategy together with the non-vector space (NVS) navigation approach. As a demonstration, the proposed nanometrology was conducted on a specific AFM platform to unravel its positioning property.**

I. INTRODUCTION

Atomic force microscopy (AFM) based manipulation technologies have been playing irreplaceable roles in fields such as NEMS fabrication, ultrahigh precision manufacturing and biological studies, thanks to abundant of measurement and manipulation options [1]–[3]. It is noted that though the AFM possesses capability of nanometer level imaging resolution, it is hard to achieve nanometer locating precision due to its tip positioning deviation ranging from serval to hundreds nanometers (depending on system status and environment). The tip locating variability is mainly caused by thermal drift [4]–[9], which distorts AFM images during the relatively long capturing time (typically, several to dozens of minutes). Since an AFM image is typically utilized as a reference map for conducting measurement and operation [9], [10], the inaccurate long-time captured image introduces location deviation to the real sample features, and consequently resulting in uncertain operation or measurement results [5], [9]. It should be noted that although positioning variability is relatively small compared to the imaging scale, it becomes really significant when nanometer or even sub-nanometer precision is required for specific applications, such as the characterization of nanowire electrical properties (typically, positioning variance should be lower than $25-50\,nm$ [2]), and single strand DNA sequencing (variance should be within $1\,nm$) [3]. Without knowing the system positioning variability, it is hard to evaluate experimental results correctly. Therefore, one of the most crucial AFM studies is the tip positioning variance characterization. With the variance knowledge, limit of operation precision will be clear and the regarding accuracy enhancement strategy can be made.

Studies on evaluating and compensating AFM positioning capability have been conducted for decades [4]–[9]. Specifically, the local scan strategies have drawn lots of attentions due to their fast positioning capability. Although AFM tip positioning error can be evaluated via lots of methods, in most cases, these approaches are facing flexibility problems, either because positioning properties were considered as location-independent incidents [4], [5], [11], or because they were estimated using predefined landmarks with specific shape and size [7], [9], [10], [12]. This challenge limits precise and universal evaluation of AFM tip positioning performance in general implementations.

To precisely and universally conduct quantitative characterization on AFM positioning variability, this research proposes a comprehensive approach by combining a featureless spiral local scan strategy with the non-vector space (NVS) navigation approach [13]. Briefly, when an AFM image is utilized as the reference map, the spiral local scan is performed in desired locations of the map to capture the very local information (no specific landmark is required); sequentially, the set feedback-based NVS controller will robustly and precisely steer the AFM tip to approach the selected desired location via measuring its surroundings. During the approaching process, the travel distance, which is performed to move the AFM probe to approach the desired location, will be recorded. This obtained

This work is supported in part by the ITF grant (GHP/040/17GD) and the ABB grant (200008545 ABB Schweiz AG). The work of L. Chen is partially supported by the grant of SZRP (JCYJ20180301171229396) and NSFC (U1613214, 61804100). The work of B. Song is partially supported by the grant of NSFC (61973294) and KRDP of Anhui Province (01904a05020086). (Equally contributed authors: Z. Sun and Y. Cheng. Corresponding authors: N. Xi, L. Chen and B. Song.)

Z. Sun and N. Xi are with Department of Industrial and Manufacturing Systems Engineering, The University of Hong Kong, Pokfulam, Hong Kong SAR {sunzy, xining}@hku.hk

Y. Cheng and Y. Yang are with Department of Electrical and Computer Engineering, Michigan State University, East Lansing, MI, 48824, USA {chengyu9, ylyang}@msu.edu

R. Yang is with Department of Mechanical and Materials Engineering, University of Nebraska-Lincoln, Lincoln, NE, 68588, USA ryang6@unl.edu

L. Chen is with Shenzhen Academy of Robotics, Shenzhen, Guangdong, 230031, China leon.chen@szarobots.com

B. Song and Z. Sun are with Institute of Intelligent Machines, Hefei Institute of Physical Science, CAS, Hefei, 230031, China songbo@iim.ac.cn

travel distance describes positioning deviation between the locally scanned image and the selected counterpart from the reference map (the large image obtained via commercial AFM software). In this manner, the tip locating variability can be calculated, which is location-dependent.

Compared to the prevalent image-based location estimation approaches, e.g. local features matching method [6], cross-correlation method [5], or visual servoing approach [14], the proposed location detection method is capable of avoiding disturbance, data missing and distortion problems generated from complicated native environment in light of the merits of NVS approach which relies only on partial local information [13]. Therefore, the AFM tip lateral positioning deviation can be estimated more precisely and reliably.

The remaining contents are arranged as follows: Section II demonstrates the positioning challenge posed by the drift along AFM lateral directions. Section III elaborates the nanometrology method. Section IV conducts the experimental study and analysis. Conclusions are summarized in the section V.

II. DRIFT INDUCED POSITIONING VARIABILITY

Thermal drift is one of the most critical factors that induce positioning deviation to AFM systems by affecting the input-output relation of their piezoelectric actuators or even fooling the feedback sensors [4]–[8]. As shown in Fig. 1 (a) and (b), a sequence of images were continuously captured via closed-loop AFM (Dimension ICON, Bruker Inc., Santa Barbara, CA, US) with commercial imaging software for more than 9 hours since the engagement. By observing the dotted-circle marked locations shown in Fig. 1 (a) and (b), it is not difficult to distinguish the shift of the location even after a relatively long imaging time.

As estimated, the maximum shift along X-axis is more than 400 nm, which is significant deviation for a $1\,\mu m \times 1\,\mu m$ imaging area. Since the X/Y-axes are well controlled and maintained in the desired region, and the sample is well fixed, the main factors attributing to the severe drift should be the unsupervised parts of the AFM physical system, such as the probe cantilever, which bends gradually due to the laser thermal during long time scanning process [8], [15]. Although the location shift caused by thermal drift poses a challenge to the long-time AFM measurement and manipulation, it can be relatively easily observed and predicted to conduct further reduction [5], [7], [10]. Compared to the obvious location shift induced by long-time thermal drift, the local positioning variance (probably induced by environmental vibration, humidity variation, AFM probe abrasion and contamination, and also noise in the feedback loop) is much more difficult to observe and predict due to its stochastic essence, thus poses a serious challenge to the high precision goal of AFM-based nanotechnology.

III. NVS CONTROL-BASED NANOMETROLOGY

Longer imaging time will definitely increase the drift effect and thus induce larger positioning error. To reduce drift influence for precisely characterizing AFM tip locating variability, a local scan-based nanoscale metrological method is proposed, the main technologies of which are elaborated as following.

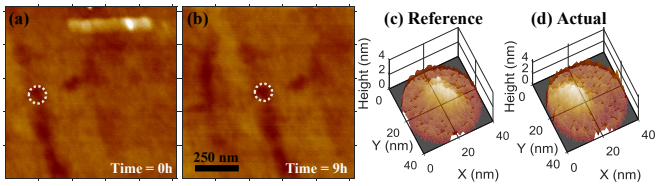

Fig. 1. Feature shift observed in global images (marked with dotted circle) and local images, (a) global image captured at the beginning, (b) global image captured after 9 hours, (c) local image with its center at the selected location of a global reference image (1024×1024 pixels, captured with raster scan taking $1280\,sec$), and (d) locally scanned image at the selected location (41×41 pixels, captured with spiral local scan taking around $4\,sec$).

A. Spiral local scan strategy

Different from the landmark-based local scan approaches [9], [10], this research developed a featureless spiral local scan strategy to perform fast imaging action on local area of the sample to reduce drift influence. Spiral pattern is known to be pretty suitable for AFM scanning, thanks to the merits of smoothness and direction-independent property [16]. The local scanning pattern is defined as (1),

$$\begin{cases} p_x(t) = R(t)\sin(\omega t) + p_{x_0} \\ p_y(t) = R(t)\cos(\omega t) + p_{y_0} \\ R(t) = C_0 t \end{cases}, \tag{1}$$

where $[p_x(t), p_y(t)]$ represents the coordinate of the AFM tip current location; $[p_{x_0}, p_{y_0}]$ denotes the selected location from a larger AFM image which is called global reference map, serving as the center of the spiral trajectory; ω is the radian rotation velocity; $R(t)$ represents the scanning radius varying at rate C_0 with respect to time linearly. As illustrated in Fig. 1(d), the spiral local scan generated image is labelled as actual since it is immediately collected after the desired location selection. For the local image shown in Fig. 1(c), it is a selection from the global reference map (such as Fig. 2(a) which was captured through long time) and thus labelled as reference.

As can be seen from Fig. 1(c) and (d), after processed with local plane-fit and filtering technology, the locally scanned area (see Fig. 1(d)) shows pretty similar overlapped features as that contained in the selected reference image (see Fig. 1(c)). However, it should be noted that overlapped parts of the two images are not exactly the same due to the system noise, local fitting enhancement process as well as the tiny drift distortion occurring to the AFM vertical direction. This is the reason for employing the robust NVS strategy to tackle the positioning issue [13].

B. NVS control method

Via the spiral local scan strategy, data can be captured uniformly and formatted as a set for performing navigation using NVS control strategy which is a set-based calculation method. When one location is chosen from a global reference map (marked with "+" in Fig. 2(a)), the local image (represented as a set mathematically) with respect to this location will be sent to the NVS controller, and the AFM tip will be steered to approach the very location with local image closest to the selected one. The travel distance along lateral directions during

the approaching process is the tip locating deviation of the selected point.

Similar to controllers developed in the vector domain, which requires control error to plan the next action, the NVS control law also depends on control error defined as the set distance (image difference). To describe difference between two sets, the Hausdorff distance is employed, which has been successfully utilized in various NVS versions [13]. The NVS control law $u(t) \in \mathbb{R}^2$ is commonly formulated as (2) derived from Lyapunov function (3) based on the set mutation analysis and the regarding element dynamics (4),

$$u(t) = \gamma(K,\hat{K}) = -\alpha D(K,\hat{K})^{+} V(K,\hat{K}), \tag{2}$$

$$V(K,\hat{K}) = \frac{1}{2}\int_{K} d^2_{\hat{K}}(p)dp + \frac{1}{2}\int_{\hat{K}} d^2_{K}(q)dq, \tag{3}$$

$$\dot{p}(t) = L(p)u(t) \text{ with } p = [p_x, p_y, h(p_x,p_y)]^T \in K, \tag{4}$$

where $h(\cdot) \in \mathbb{R}^N$ represents the local data associated with central location $[p_x, p_y]$; $L(p) = [I_{2\times 2}, -\nabla h \Lambda]^T$ with $I_{2\times 2}$ denoting the identity matrix, $\Lambda \in \mathbb{R}^{N\times N}$ being the selection matrix, and $\nabla = [\partial/dp_x, \partial/dp_y]^T$ representing gradient at location $[p_x, p_y]$; K and $\hat{K}$ represent the obtained image (in the set form) via local scan and the selected one from the global reference map, respectively; $d_{\hat{K}}(p)$ is defined as $\min_{q\in\hat{K}} \|p-q\|_2$ denoting distance between element p to set $\hat{K}$; α is the gain to regulate control strength which determines the approaching speed; $D(K,\hat{K})^{+}$ is the pseudo-inverse of $D(K,\hat{K})$ defined as (5),

$$\begin{aligned} D(K,\hat{K}) = &\frac{1}{2}\int_{K} d^2_{\hat{K}}(p)\Big(\sum_{i=1}^{N+2}\frac{\partial L_i}{dp_i}\Big)^T dp + \int_{K} L(p)^T(p- \\ &\Pi_{\hat{K}}(p))dp - \int_{\hat{K}} L(\Pi_K(q))^T(q-\Pi_K(q))dq, \end{aligned} \tag{5}$$

where L_i represents the i^{th} row of matrix L; $\Pi_{\hat{K}}(p) = \{q : \|p-q\|_2 = d_{\hat{K}}(p) \text{ with } q \in \hat{K}\}$ is a function to map p to associated element in the set $\hat{K}$.

Based on the control law $u(t)$, the local scan collected image K approaches the selected $\hat{K}$ exponentially fast, and the lateral positioning deviation thus can be calculated as $\int_{t_0}^{t} G[u(\tau)]d\tau$, where $G[\cdot]$ represents the function for mapping the control effect $u(\cdot)$ to AFM tip travel distance. For a lateral closed-loop AFM, $G[\cdot] = -I_{2\times 2}$.

IV. EXPERIMENTAL STUDY AND ANALYSIS

In this research, an ICON AFM with customer-control system and standard ScanAssist-Air probe with peakforce tapping (PFT) imaging mode were utilized to reveal the property of tip locating variability. The physical system is comprised of the ICON AFM; one AFM PC for running the commercial software; one user interface PC with DAQ card (NI-PCI-6221) and customer-control system installed; a haptic joystick (Geomagic 3D Touch Stylus) for sending haptic feeling to and receiving command from the users. During all the experiments, the AFM system was kept in a hood with environmental temperature between 24.2 to 24.4 $^{\circ}C$, and the system was warmed up for at least 8 hours since the engagement. Without specific description, global reference images were all taken with 1024×1024 pixels using $1280\,sec$, and the spiral local scan images were captured with 41×41 pixels using $4\,sec$.

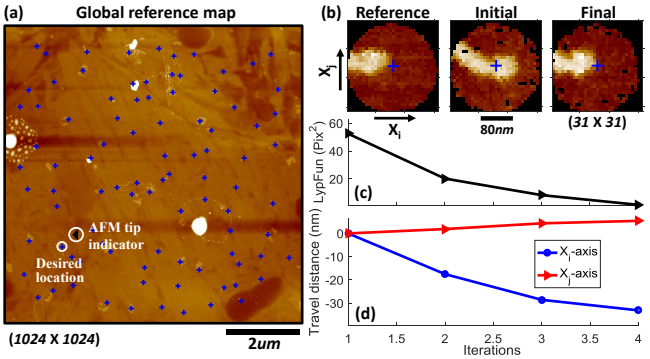

Fig. 2. Measurement of AFM tip lateral positioning deviation using NVS-based navigation method, (a) the global reference map with selected locations (marked by "+" symbols), (b) typical desired location approaching result illustrated as local images, (c) corresponding convergence of NVS positioning error (Lyapunov function), and (d) estimated travel distance of AFM tip.

A. Demonstration of NVS-based nanometrology

During the AFM positioning variability characterization experiment, locations marked with "+" were selected manually from the global reference map (as shown in Fig. 2(a)) by the user via the haptic joystick (indicated as a triangle symbol in Fig. 2(a)) to generate reference images for NVS navigation. Subsequently, the spiral local scan was performed to reveal the local information at the actual location, and then the AFM tip was driven by the NVS controller to move towards the selected location. When the image difference (set distance) is less than a predefined threshold (e.g. one pixel), the NVS controller stops approaching the current reference image and continues to steer the AFM tip to approach the next. Typical NVS control results are shown in Fig. 2(b)-(d). From images of (b), one can see the image at the initial location is very different from that of the desired location (marked in Fig. 2(a)) at the beginning. After steered by the NVS strategy, the locally captured image finally matched the desired one (convergence of the regarding Lyapunov function is shown in Fig. 2(c)), which means the current location is pretty close to the desired location. During the approaching process, the AFM tip travel distance was captured via the AFM lateral sensors, and the positioning deviation of the selected location is the last point of the curves shown in Fig. 2(d).

B. AFM lateral positioning variability characterization

During the variability characterization experiment, three groups of tests were conducted, including imaging with 0°, 45° and 90° rotation angle, respectively. For each rotation angle, AFM images with the scan-size $2\,\mu m$, $5\,\mu m$ and $10\,\mu m$ were captured, respectively; subsequently, around 100 locations (marked with "+" in Fig. 3 (a)-(c)) were manually selected for each image, and the regarding positioning deviation was precisely measured using the proposed nanometrology; finally the travel distance corresponding to each location was collected and summarized in Fig. 3(d)-(i) (typical results).

In Fig. 3, the mean values for the fast and slow axis are the averaged positioning error between the reference locations and the actual locations. From the results one can see the measured deviation distributions are all with offsets, which are

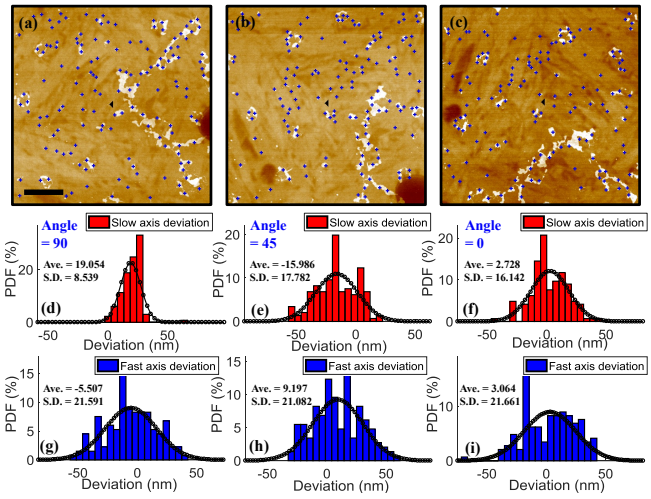

Fig. 3. Typical results of AFM positioning variability characterization (scale bar: $1\,\mu m$), (a) global reference map scanned with 90° rotation angle, (b) 45° rotation angle, (c) 0° rotation angle, (d) fast axis positioning error distribution of 90° image, (e) fast of 45°, (f) fast of 0°, (g) slow axis positioning error distribution of 90° image, (h) slow of 45°, (i) slow of 0°.

corresponding to the image shift induced by the thermal drift during the relatively long imaging time. It is noted that the distributions shown in Fig. 3(d)-(i) are not pretty consistent, this should be induced by the combined effect of the AFM scanner directional property and the tip profile. Assume that an AFM tip has a wider radius at one direction, then it will be harder to distinguish the measured location from its very close neighbourhood along this direction, consequently resulting in a narrower distribution. It is also interesting to see the fast axis standard deviation is always larger than that of the slow axis in the three rotation scenarios, respectively. By comparing the distribution (d) and (i) (or (f) and (g)), which are corresponding to the same physical scanner axis, one can see that the faster scanning velocity can introduce more positioning variability when the imaging resolution is fixed. This phenomenon was also observed in the tests with different scanning scales, and the results are summarized in Fig. 4, which also suggest that narrower scanning scale guarantees lower positioning variability when the imaging resolution is fixed. It should be noted that the pixel-size factor influences the characterization results in Fig. 4, but it is pretty limited since sub-pixel measurement accuracy can be guaranteed by the NVS control-based nanometrology.

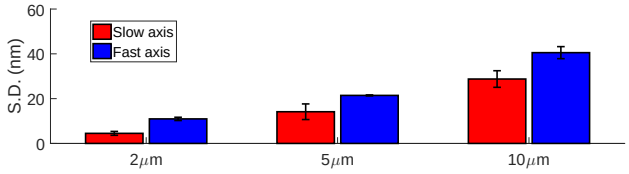

Fig. 4. Comparison of standard deviation of positioning deviation distribution among the scan-size: $2\,\mu m$ (pixel-size: $\sim 2.0\,nm$), $5\,\mu m$ (pixel-size: $\sim 4.9\,nm$) and $10\,\mu m$ (pixel-size: $\sim 9.8\,nm$).

V. CONCLUSION

In this study, the spiral local scan-based NVS nanometrological approach is proposed to perform precise AFM lateral positioning variability characterization. Spiral pattern possesses merits such as smoothness and direction-independent property, thus efficient for imaging at local area. The NVS method is based on set calculation, which is independent of system coordinate, thus it is a natural way to tackle distorted AFM data without exact coordinate. Therefore, the spiral local scan-based NVS nanometrology is a pretty promising tool for performing precise measurement at the nanoscale. Based on the nanometrology, comprehensive modelling of AFM tip positioning variability can be developed in the future, which will consider various factors, such as the ambient temperature, scan-size, imaging resolution as well as the tip profile.

REFERENCES

[1] G. Binnig, C. F. Quate, and C. Gerber, "Atomic force microscope," *Physical review letters*, vol. 56, no. 9, p. 930, 1986.

[2] X. Zhou, S. Dayeh, D. Aplin, D. Wang, and E. Yu, "Direct observation of ballistic and drift carrier transport regimes in inas nanowires," *Applied Physics Letters*, vol. 89, no. 5, p. 053113, 2006.

[3] Z. He, Z. Han, M. Kizer, R. J. Linhardt, X. Wang, A. M. Sinyukov, J. Wang, V. Deckert, A. V. Sokolov, J. Hu *et al.*, "Tip-enhanced raman imaging of single-stranded dna with single base resolution," *Journal of the American Chemical Society*, vol. 141, no. 2, pp. 753–757, 2018.

[4] R. Staub, D. Alliata, and C. Nicolini, "Drift elimination in the calibration of scanning probe microscopes," *Review of scientific instruments*, vol. 66, no. 3, pp. 2513–2516, 1995.

[5] B. Mokaberi and A. A. Requicha, "Drift compensation for automatic nanomanipulation with scanning probe microscopes," *IEEE Transactions on Automation Science and Engineering*, vol. 3, no. 3, pp. 199–207, 2006.

[6] S. Belikov, J. Shi, and C. Su, "Afm image based pattern detection for adaptive drift compensation and positioning at the nanometer scale," in *American Control Conference, 2008*. IEEE, 2008, pp. 2046–2051.

[7] G. Li, Y. Wang, and L. Liu, "Drift compensation in afm-based nanomanipulation by strategic local scan," *IEEE Transactions on Automation Science and Engineering*, vol. 9, no. 4, pp. 755–762, 2012.

[8] T. R. Meyer, D. Ziegler, C. Brune, A. Chen, R. Farnham, N. Huynh, J.-M. Chang, A. L. Bertozzi, and P. D. Ashby, "Height drift correction in non-raster atomic force microscopy," *Ultramicroscopy*, vol. 137, pp. 48–54, 2014.

[9] S. Yuan, Z. Wang, L. Liu, N. Xi, and Y. Wang, "Stochastic approach for feature-based tip localization and planning in nanomanipulations," *IEEE Transactions on Automation Science and Engineering*, vol. 14, no. 4, pp. 1643–1654, 2017.

[10] L. Liu, Y. Luo, N. Xi, Y. Wang, J. Zhang, and G. Li, "Sensor referenced real-time videolization of atomic force microscopy for nanomanipulations," *IEEE/ASME Transactions on Mechatronics*, vol. 13, no. 1, pp. 76–85, 2008.

[11] Q. Yang, S. Jagannathan, and E. W. Bohannan, "Automatic drift compensation using phase correlation method for nanomanipulation," *IEEE Transactions on Nanotechnology*, vol. 7, no. 2, pp. 209–216, 2008.

[12] E. Tranvouez, E. Boer-Duchemin, G. Comtet, and G. Dujardin, "Active drift compensation applied to nanorod manipulation with an atomic force microscope," *Review of Scientific Instruments*, vol. 78, no. 11, p. 115103, 2007.

[13] B. Song, Z. Sun, N. Xi, R. Yang, Y. Cheng, L. Chen, and L. Dong, "Enhanced nonvector space approach for nanoscale motion control," *IEEE Transactions on Nanotechnology*, vol. 17, no. 5, pp. 994–1005, 2018.

[14] T. Xu, Y. Guan, J. Liu, and X. Wu, "Image-based visual servoing of helical microswimmers for planar path following," *IEEE Transactions on Automation Science and Engineering*, 2019.

[15] F. Marinello, P. Bariani, L. De Chiffre, and E. Savio, "Fast technique for afm vertical drift compensation," *Measurement Science and Technology*, vol. 18, no. 3, p. 689, 2007.

[16] M. Rana, H. Pota, and I. Petersen, "Spiral scanning with improved control for faster imaging of afm," *IEEE Transactions on Nanotechnology*, vol. 13, no. 3, pp. 541–550, 2014.